

This article was downloaded by:

On: 30 January 2011

Access details: *Access Details: Free Access*

Publisher *Taylor & Francis*

Informa Ltd Registered in England and Wales Registered Number: 1072954 Registered office: Mortimer House, 37-41 Mortimer Street, London W1T 3JH, UK



International Journal of Polymeric Materials

Publication details, including instructions for authors and subscription information:

<http://www.informaworld.com/smpp/title~content=t713647664>

DSC Study of Syndiotactic Polypropylene/Organoclay Nanocomposite Fibers: Crystallization and Melting Behavior

Eberhard Borsig^{ab}; Anna Ujhelyiová^a; Zita Mlynarčíková^a; Dirk Kaemfer^c; Rolf Mülhaupt^c; Anton Marcinčin^a; Dušan Berek^b

^a Institute of Polymer Material, Faculty of Chemical and Food Technology, Slovak University of Technology in Bratislava, Bratislava, Slovakia ^b Polymer Institute, Slovak Academy of Science, Bratislava, Slovakia ^c Freiburger Materialforschungszentrum und Institut für Makromolekulare Chemie der Albert-Ludwigs Universität, Freiburg, Germany

To cite this Article Borsig, Eberhard , Ujhelyiová, Anna , Mlynarčíková, Zita , Kaemfer, Dirk , Mülhaupt, Rolf , Marcinčin, Anton and Berek, Dušan(2007) 'DSC Study of Syndiotactic Polypropylene/Organoclay Nanocomposite Fibers: Crystallization and Melting Behavior', *International Journal of Polymeric Materials*, 56: 8, 771 – 788

To link to this Article: DOI: 10.1080/00914030601163399

URL: <http://dx.doi.org/10.1080/00914030601163399>

PLEASE SCROLL DOWN FOR ARTICLE

Full terms and conditions of use: <http://www.informaworld.com/terms-and-conditions-of-access.pdf>

This article may be used for research, teaching and private study purposes. Any substantial or systematic reproduction, re-distribution, re-selling, loan or sub-licensing, systematic supply or distribution in any form to anyone is expressly forbidden.

The publisher does not give any warranty express or implied or make any representation that the contents will be complete or accurate or up to date. The accuracy of any instructions, formulae and drug doses should be independently verified with primary sources. The publisher shall not be liable for any loss, actions, claims, proceedings, demand or costs or damages whatsoever or howsoever caused arising directly or indirectly in connection with or arising out of the use of this material.

DSC Study of Syndiotactic Polypropylene/Organoclay Nanocomposite Fibers: Crystallization and Melting Behavior

Eberhard Borsig

Institute of Polymer Material, Faculty of Chemical and Food Technology, Slovak University of Technology in Bratislava, Bratislava, Slovakia and Polymer Institute, Slovak Academy of Science, Bratislava, Slovakia

Anna Ujhelyiová Zita Mlynarčíková

Institute of Polymer Material, Faculty of Chemical and Food Technology, Slovak University of Technology in Bratislava, Bratislava, Slovakia

Dirk Kaemfer Rolf Mülhaupt

Freiburger Materialforschungszentrum und Institut für Makromolekulare Chemie der Albert-Ludwigs Universität, Freiburg, Germany

Anton Marcinčin

Institute of Polymer Material, Faculty of Chemical and Food Technology, Slovak University of Technology in Bratislava, Bratislava, Slovakia

Dušan Berek

Polymer Institute, Slovak Academy of Science, Bratislava, Slovakia

The effect of anisotropic particles of organophilic layered silicate on the crystallization and melting behavior of prepared nanocomposite systems was studied. The matrix was syndiotactic polypropylene (sPP). Organophilic layered silicate M-QDA filler was prepared by modification of hectorite SOMASIF ME 100 with octadecyl amine. The compatibilizer was isotactic polypropylene (iPP) grafted with maleic anhydride (iPP-g-MA). The silicate was exfoliated in situ within the

Received 14 November 2006; in final form 28 November 2006.

Support was received from the FP6 project: NMP3-CT-2005-516972 NANOHYBRID.

Address correspondence to Eberhard Borsig, Institute of Polymer Material, Faculty of Chemical and Food Technology, Slovak University of Technology in Bratislava, Radlinskeho 9,81237 Bratislava, Slovakia. E-mail: eberhard.borsig@stuba.sk

sPP during the melting process to produce anisotropic nanoparticles. The sPP/M-ODA nanocomposite was spun at different drawing ratios. The resulting fibers were examined by differential scanning calorimetry. It was found that neither the spinning process nor the presence of nanofiller affected the crystallinity of the sPP matrix of the nanocomposite in comparison with the neat sPP. At a raised drawing ratio of the fibers slightly increased crystallinity of matrix was observed; however, it was still lower than the neat sPP fibers prepared at the same drawing ratio. The presence of M/ODA nanofiller in sPP matrix increased the melting temperature of the fibers.

Keywords: fibers, nanocomposite, organoclay, polypropylene

INTRODUCTION

Recently, studies of polyolefin/organoclay systems were extended to new systems of syndiotactic polypropylene/organoclay nanocomposites [1–2]. Improvement is expected in some mechanical properties like strength or impact resistance. Although syndiotactic polypropylene (sPP) has been known since the work of Natta et al. [3–4], its physical properties have been more intensively investigated only in the last decade [4–12]. Polymorphism in the solid-state structure of sPP has been identified. According to the latest literature data, syndiotactic polypropylene crystallizes in four different forms [9,13]. The most stable, and by far best-understood crystalline morphology, commonly known as form I, is composed of helical polymer chains packed in an orthorhombic lattice. This form was obtained most readily by slow crystallization of highly syndiotactic material from the melt at elevated temperature [4–13]. When crystallized at lower temperatures-below 12°C-polymer chain helices lay adjacent to one another along both the a axis and b axis. Form II is obtained more readily from sPP of lower stereo-regularity content [10,13]. Its formation is influenced by chain alignments taking place during annealing as well as by mechanical forces on the sPP melt [13–15]. Crystalline form III is a meta-stable sPP polymorph composed of all-trans-planar zig-zag chains in orthorhombic unit cells. Also, longer residence times at 0°C increase the stability of the trans-planar mesomorphic phase, which remains stable and inhibits the normal crystallization of the sample into the helical form at room temperature. This has been observed in sPP films quenched from the melt and subsequently drawn at 0°C [11]. Form IV, the least well known of the four crystalline structures of sPP, is arranged in a triclinic unit cell. This polymorph was obtained upon exposing quenched, cold drawn sPP films, rich in form III, to appropriate solvent vapors (benzene, toluene, or

p-xylene) for several days [13]. Films and fibers of sPP have exhibited highly elastomeric behavior during mechanical testing [14–15], which also has been observed in the authors' previous work [2]. Deformation-induced morphology changes are thought to be responsible for the elasticity [14–15]. De Rosa and co-workers [10] have demonstrated that non-deformed films, which were rich in form I crystals and subjected to strains much greater than 400%, have become rich in form III crystals. This observation suggests a change in overall chain conformation (from helical to planar zig-zag) [13]. Strobl et al. have found that the crystallinity after isothermal crystallization processes remains invariant over wider temperature ranges, thus demonstrating that the potential of the entangled melt to form crystals is a well-defined property [6]. It is expected that the morphology changes in sPP caused by mechanical deformation, and also in the presence of nanoparticles, would influence the thermal behavior of sPP matrix.

The crystallization process of sPP is also influenced by some other factors. Variation of crystallization temperature usually leads to a change in the crystalline layer thickness [13]. It was found that the amount of helical form I of sPP in the sPP/clay nanocomposites increased during the UV cold irradiation of the specimens, whereas the amount of segments characterized by trans planar conformation decreased [16]. Concerning the nucleating efficiency of the nanoparticles, it was found that the extinction coefficient decreased as the particle size dropped. This leads to a decrease of the optical density and increase in the transparency for nanoparticle-filled sPP. Increase of transparency could be associated with two factors: (a) smaller crystallite size of calcium phosphate at high concentration of polyethylene-oxide, and (b) high crystallization rate of sPP in presence of nanoparticles leading to a very small spherulite size [17].

In this article, differential scanning calorimetry (DSC) is used to examine the influence of anisotropic nanoparticles on crystallization and melting behavior of sPP fibers. The nanoparticles were generated in sPP during melt processing by means of in situ exfoliation of organophilic layered silicate (M-ODA). The influence of the spinning process on the crystallinity of sPP/organoclay nanocomposite fibers was also investigated.

EXPERIMENTAL

Materials

Syndiotactic polypropylene (sPP) in the form of thermally stabilized granules, and identified as FINA 96-30, was a product of the firm Fina,

La Porte, Texas, USA. FINA 96-30 was used as polymeric matrix of the nanocomposite. Its melting temperature (T_m) = 130°C, density $\rho = 0.88 \text{ g.cm}^{-3}$ and melt flow-index (MFI) was 4 g/10 min. According to the supplier FINA 96-30 exhibited relatively narrow molecular weight distribution: $M_w = 180,000 \text{ g.mol}^{-1}$, $M_n = 72,000 \text{ g.mol}^{-1}$, $M_w/M_n = 2.5$.

The filler was a synthetic clay, fluorohectorite, produced by CO-OP Chemical CO., Japan. Under trade name SOMASIF ME 100. It was obtained by heating talcum in presence of Na_2SiF_6 . This material was subsequently treated with protonated octadecylamine (M-ODA), as reported in detail elsewhere [1]. The compatibilizer used was isotactic polypropylene (iPP) grafted with maleic anhydride (iPP-g-MA). It was a product of Clariant (Huninque, France). Compatibilizers with lower molar mass ($M_n = 2900 \text{ g.mol}^{-1}$ and $M_w = 11890 \text{ g.mol}^{-1}$), containing 3.5 wt% MA groups (Licomont AR 504), and with higher molar mass ($M_n \approx 7500 \text{ g.mol}^{-1}$) containing 4.2 wt% of MA groups (Hostaprime HC5) were investigated.

Composite Preparation

All composites were prepared under identical mixing and molding conditions. The weight fractions of filler M-ODA and compatibilizer were varied between 1 and 4 wt% for Licomont AR 504 and between 1 and 7 wt% for Hostaprime HC5. sPP powder and the organoclay were premixed with the stabilizers – 0.2 wt% Irganox 1010/Irgafos 168 (4/1 wt%) and the iPP-g-MA. Melt blending was performed in a co-rotating twin-screw extruder (Collin; ZK 25 T) at 190–230°C and at 120 rpm. The obtained strands were pelleted and dried at 80°C.

Spinning of the sPP/Organoclay Nanocomposite

The pelleted sPP nanocomposite was spun in a laboratory spinning machine manufactured by VUCHV (Svit, Slovakia). The essential spinning conditions included a spinning speed of 49 m.min^{-1} using an extruder with screw diameter of 16 mm and length of 112 cm and homogenization temperature of 280°C. Thirteen spinnerets of 0.05 mm diameter produced fibers that were partially oriented, and these fibers were drawn at 70°C at one of three drawing ratios: $\lambda = 1, 2, \text{ or } 3$.

Thermal characteristics of sPP/SOMASIF nanocomposite fibers were evaluated by a DSC 7 apparatus Perkin Elmer (Norwalk, Conn., USA) using the following procedure: A sample of the original fiber was heated at a rate of 10 K.min^{-1} from 50°C to 220°C. Thus, a melting endotherm of the original sample with melting temperatures, T_{m1} ,

and melting enthalpy, ΔH_{m1} – after first heating was obtained. Then the sample was cooled at the rate of $50 \text{ K}\cdot\text{min}^{-1}$ to obtain the crystallization exotherm with crystallization temperature, T_c , and crystallization enthalpy, ΔH_c . Subsequently, the sample was exposed to a second heating at a rate of $10 \text{ K}\cdot\text{min}^{-1}$ to determine the endotherm with a melting point, T_{m2} , and enthalpy. Measurements were performed under nitrogen atmosphere.

The calculated melting enthalpy ΔH_{calc} is related to the measured enthalpy $\Delta H_{\text{exp},0}$ of the neat sPP (fiber) by taking into account that the weight fraction of sPP in the nanocomposite is $(1 - W_{\text{ad}})$:

$$\Delta H_{\text{calc}} = \Delta H_{\text{exp},0}(1 - W_{\text{ad}}) \quad (1)$$

where W_{ad} is the weight fraction of additives in nanocomposite.

RESULTS AND DISCUSSION

Generally, the structure and mechanical properties of the fibers prepared from a given polymer or polymer system are considerably influenced by the conditions of their preparation and also by the presence of additives utilized. These conditions are directly related to the formation of the crystalline fraction in the polymer fibers [9]. Thermal behavior and extent of crystallinity in nanocomposite fibers of the system syndiotactic polypropylene/synthetic clay (sPP/M-ODA) were determined using differential scanning calorimetry (DSC). It was possible to utilize the crystallization enthalpy change, ΔH_c , and relate it to the data about the sPP crystalline fraction in the given systems. The values of thermal characteristics were obtained for samples of sPP nanocomposite fibers with constant content of the filler, M-ODA (4 wt%, Table 1) and for various contents of the compatibilizer, Licomont AR 504, in the range from, 2.5 to 7.5 wt%. For these samples, thermograms from the first and the second annealing were obtained. The first annealing resulted in the destruction of the supermolecular structure in the sPP nanocomposite fibers, which arose during spinning and drawing. The thermograms of the second annealing correspond to the crystallization.

Thermograms of the first annealing of unfilled sPP and nanocomposite fibers showed a large peak (majority peak) in a melting temperature region of $125\text{--}128^\circ\text{C}$, and the second, a small peak (minority peak) in the region of $150\text{--}162^\circ\text{C}$ (Figure 1).

The melting temperatures of the majority peak of all studied sPP nanocomposite fibers, prepared at $\lambda = 1$ —except of Sample 11—were slightly higher than that of the neat sPP fibers prepared under the

TABLE 1 Melting Temperature of sPP Matrix of the Selected Samples of sPP Nanocomposite Fibers at Their First Annealing

Sample No.	Filler M-ODA wt%	Compatibilizer (iPP-g-MA) wt%	Drawing ratio λ	T_{m1} °C	
0	—	100	—	152,6	—
1	—	—	1	125,5	162,1
7	1,5	5	1	125,7	150,0
11a	2,5	5	1	127,3	150,0
17	4	—	1	125,9	161,4
14a	4	2,5	1	128,1	157,9
15a	4	5	1	127,0	148,8
16	4	7,5	1	128,4	150,5
22a*	4	5	1	127,0	150,1
11b	2,5	5	3	124,4	153,2
14b	4	2,5	3	126,9	157,5
15b	4	5	3	126,6	149,8
22b*	4	5	3	125,8	143,2

Sample: 0 is compatibilizer alone. 1 is a neat sPP. Nanocomposites marked with * contain compatibilizer iPP-g-MA having higher molecular weight (HC5).

All other samples in this Table contain compatibilizer iPP-g-MA with lower molecular weight (AR504).

same conditions. On the other hand, all melting temperatures of the second peak were lower (Table 1).

In the amorphous state, sPP possessed a considerably high number of zig-zag conformations [18]. This conformation arises at drawing of the sPP melt by the Petermann-Gohil method. The zig-zag conformations in the solid state are metastable [19]. At higher temperature, all zig-zag conformations transformed into helices as a result of the tightly arranged crystalline structure and highly arranged structural modification III, which easily arises from the drawn zig-zag chains.

The crystallization temperature of sPP lies in the region, $60 < T_c < 110^\circ\text{C}$ [7,14]. sPP crystallizes preferentially into the orthorhombic crystalline structure II. Its basic unit consists of two double-helices aligned side by side, and alternating along the axes of the chain. If the temperature is $T_c > 110^\circ\text{C}$, sPP transforms to a combination of the orthorhombic crystalline structures II and III, in which double-helices alternate along the axes a and b. Unlike modification II, modification III arose only after very long crystallization time under normal isothermal conditions of crystallization. However, by uniaxial drawing of the sPP samples, a modification III can be obtained also at short crystallization time and under normal isothermal conditions [4].

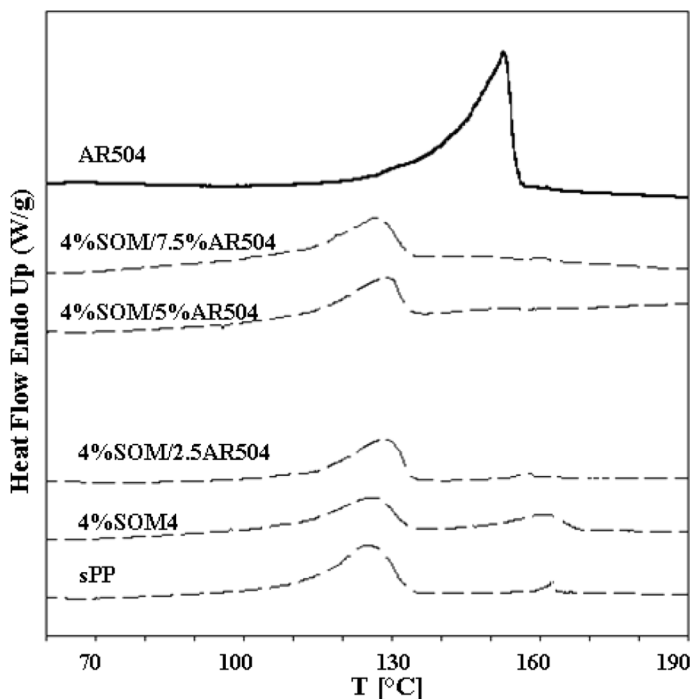


FIGURE 1 DSC Thermograms of neat sPP, compatibilizer AR504 alone and sPP nanocomposite fibers with constant content of the filler M-ODA = 4 wt% and various content of the compatibilizer AR504; 2.5; 5 and 7.5 wt% resp. at the first annealing.

On the basis of this knowledge, the majority peak of the thermogram from the first annealing of the sPP nanocomposite fibers ($T_{m1} = 125\text{--}128^\circ\text{C}$) was assigned to the structural modification II of sPP chains and the minority peak ($T_{m1} \sim 160^\circ\text{C}$) was assigned to the structural modification III of the sPP chains (Figure 1).

The minority peak, which corresponds to melting temperature for sPP of 162.1°C , was shifted toward lower temperatures as a consequence of the increase in content of the compatibilizer AR 504 of lower molecular weight (All samples contained constant content of the filler ~ 4 wt%, Figure 1).

The melting temperatures of the iPP individual crystalline modifications are as follows: α -modification: $162\text{--}166^\circ\text{C}$; mixed α - β -modification: $154\text{--}159^\circ\text{C}$; β -modification: 152°C and γ -modification: 120°C . On the assumption, that iPP-g-MA crystallizes in the same modifications as iPP, the shifts of sPP peaks from $T_{m1} = 162.1^\circ\text{C}$ to $T_{m1} = 150^\circ\text{C}$ (Table 1)

can be explained by the formation of a mixed modification III sPP and α - β -modification of iPP. The minority peaks on the thermograms are very small and expressionless, which can be caused by the low content of the compatibilizer AR504 in comparison to the sPP.

All melting enthalpies ΔH_{m1} of the nanocomposite fibers obtained from DSC measurements (Table 2, column A) were lower than those of the neat sPP fibers. This means that the additives, that is, filler and compatibilizer did not support an increase of the sPP crystallinity. The values ΔH_{m1} at the same composition of composite but prepared at higher drawing ratio $\lambda = 3$ were usually higher than those prepared at $\lambda = 1$. The same result was observed also for fibers with the compatibilizer of higher molar mass HC5 (Samples 22*a, and 22*b, (Table 2). It means that the nanofiller does not support an increase in amount of sPP modification II. However, when fibers were prepared at higher drawing ratio the formation of sPP modification II was higher. Thus, orientation of nanocomposite fibers increased their crystallinity; however, the latter was still lower than in the neat sPP fibers.

The decrease of sPP matrix crystallinity in the nanocomposite fibers can be understood as a result of the competition between formation of

TABLE 2 Melting Enthalpies of the Selected Samples of sPP Nanocomposites at the First Annealing

Sample no.	M-ODA wt%	iPP-g-MA wt%	Drawing ratio λ	ΔH_{m1} , J.g ⁻¹					
				A		B			
				exp	calc	exp	calc	exp	
0	—	100							72,6
1	—	—	1	27,2	—	1,0	—	—	—
7	1,5	5	1	23,6	25,4	1,3	0,94	—	—
11a	2,5	5	1	23,7	25,2	1,2	0,93	—	—
17	4	—	1	15,5	26,1	5,8	0,96	—	—
14a	4	2,5	1	26,3	25,4	0,9	0,94	—	—
15a	4	5	1	17,8	24,8	0,9	0,91	0,3	—
16	4	7,5	1	23,3	24,1	0,8	0,89	—	—
22a*	4	5	1	17,1	24,8	0,9	0,91	—	—
11b	2,5	5	3	26,2	—	4,0	—	—	—
14b	4	2,5	3	26,2	—	0,1	—	—	—
15b	4	5	3	25	—	0,5	—	—	—
22b*	4	5	3	22,8	—	0,2	—	—	1,0

Sample: 0 is compatibilizer alone. 1 is a neat sPP. Nanocomposites marked with* contain compatibilizer iPP-g-MA having higher molecular weight (HC5).

All other samples in this Table contain compatibilizer iPP-g-MA with lower molecular weight (AR504).

a physical network formed in the amorphous part of sPP caused by the nanoparticles, and crystallization of the free sPP chains.

Samples 22a and 22b containing the compatibilizer HC5, differed from sample 15, only in molar mass of compatibilizer (Table 1). All these samples were of the same composition, that is, they contained 4 wt% of filler M-ODA and 5 wt% of the compatibilizer. The displayed thermogram of sample 22a containing compatibilizer HC5 differed from sample 15 only in having a third peak, which was observed in the temperature region 155–165°C. The melting temperatures and melting enthalpies of both samples were very similar to α - β modification of iPP (Tables 1 and 2), but the sample 22b containing HC5 prepared at higher drawing ratio $\lambda = 3$ showed also a third peak, which can be a mixed modification III of sPP [5,7].

The experimentally measured enthalpy ($\Delta H_{\text{ml}(\text{exp})} = 15.5 \text{ J}\cdot\text{g}^{-1}$) of sample 17 containing 4 wt% of M-ODA without compatibilizer, differs from the melting enthalpy calculated for sPP in the given nanocomposite ($\Delta H_{\text{ml}(\text{calc})} = 26.1 \text{ J}\cdot\text{g}^{-1}$, Table 2, column A). The melting enthalpy of all samples at lower temperature, T_{ml} (Table 2, column A) were: $\Delta H_{\text{ml}(\text{exp})} \geq \Delta H_{\text{ml}(\text{calc})}$. For melting enthalpy at higher temperature, T_{ml} (Table 2, column B) the relationship was: $\Delta H_{\text{ml}(\text{exp})} \geq \Delta H_{\text{ml}(\text{calc})}$. Change of the melting enthalpy indicated the mutual interaction between the filler and matrix. This means that the filler suppresses formation of the sPP crystalline modification II and supports formation of modification III.

The calculated values of the melting enthalpy $\Delta H_{\text{ml}(\text{calc})}$, for sPP nanocomposites with different filler content and with constant content of compatibilizer (samples 7, 11a, and 15a) are mostly lower compared with experimental melting enthalpy values for sPP without additives. This was evident from the peak of thermograms with lower melting temperature, T_{ml} (Table 1, Figure 2).

The crystallization thermograms of the nanocomposites in Figure 3 show that samples containing 4 wt% filler and 2.5 to 7.5 wt% of compatibilizer exhibited one small peak in the temperature region 73–80°C (Tables 3 and 4). In the case of the sample without compatibilizer and with 4 wt% of filler (M-ODA), a peak at $T_c = 118.4^\circ\text{C}$ appeared (Table 3). This peak could be ascribed to the presence of structural modification III. It was also found that with increasing content of compatibilizer iPP-g-MAN, the crystallization temperature of sPP nanocomposites increased (Table 3). Obviously, the iPP, which crystallizes at a higher temperature than sPP, can act as a nucleating agent for sPP [1]. On the other hand, there should also be a better distribution of the silicate filler with increase of the compatibilizer content in the nanocomposite. This should result in a decrease of its

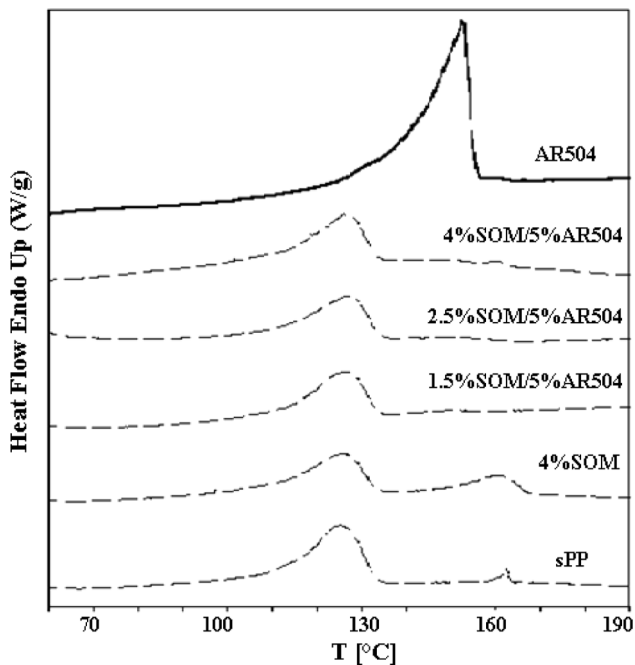


FIGURE 2 DSC thermograms of the first annealing of the sPP nanocomposite samples containing 1.5; 2.5; and 4 wt% of M-ODA and a constant content of compatibilizer AR504 = 5 wt% and thermogram of unfilled sPP (without compatibilizer and nanofiller).

nucleation activity [17]. An increase in nucleation, however, apparently did not cause a rise of crystallization temperature (Table 3). This means that the decisive role on crystallization temperature, T_c , of the sPP nanocomposite has the T_c of the compatibilizer at least at constant content of filler = 4 wt% (samples 14, 15, and 16). But the values of the ΔH_c do not change proportionally (Table 3).

It was found that with increasing content of silicate in iPP nanocomposites, the rate of spherical growth decreased [17]. The layered silicate particles lowered the rate of radial growth of lamellas. However, growth of lamellas did not stop completely, but it proceeded probably through “bridges” among silicate particles. The size of spherulites of these nanocomposites was much smaller than in neat iPP and decreased in the order: iPP > iPP/filler > iPP/filler/compatibilizer [17].

The difference between experimentally obtained melting enthalpies of sPP nanocomposites and the values calculated for various contents

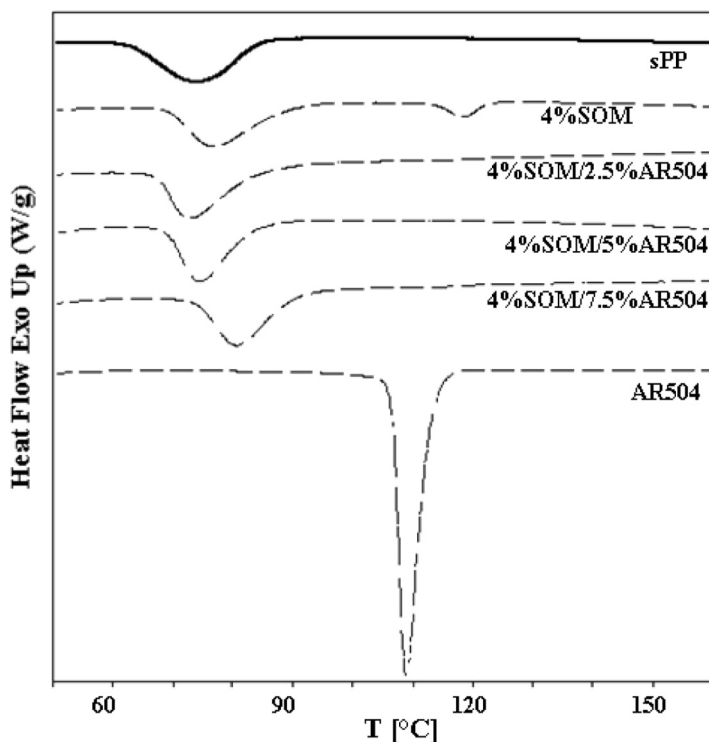


FIGURE 3 DSC Thermograms of Crystallization of: sPP without Additives; compatibilizer AR504 and sPP nanocomposite samples with constant content of the filler M-ODA = 4 wt% and with various content of the compatibilizer AR504 (2.5; 5 and 7.5 wt%).

of sPP in sPP nanocomposites shows that in the majority of cases $\Delta H_{c(\text{exp})} > \Delta H_{c(\text{calc})}$ (Tables 2 and 3). The difference between $\Delta H_{c(\text{exp})}$ and $\Delta H_{c(\text{calc})}$ for nanocomposite fibers is relatively small and it is not possible to show an unambiguous dependence of ΔH_c on the content of filler M-ODA or on the content of compatibilizer iPP-g-MAN. Only the value $\Delta H_{c(\text{exp})} = 23.7 \text{ J.g}^{-1}$ for sample 17 is much lower than the calculated one, $\Delta H_{c(\text{calc})} = 28.2 \text{ J/g}$. This agrees with the authors' previous study [17] and indicates higher amount of unexfoliated particles of the filler in sPP nanocomposite, which was prepared without compatibilizer [2]. On the other hand, unexfoliated particles are effective nucleation agents but their presence leads to the growth of smaller lamellas. For the preparation of samples where compatibilizer was added, that was primarily responsible for the exfoliation of the filler,

TABLE 3 Crystallization Temperatures and Enthalpies of the Selected Samples of sPP Nanocomposite Fibers

Sample No.	M-ODA wt%	iPP-g-MA wt%	Drawing ratio λ	T_c °C	ΔH_c J.g ⁻¹			
					(exp)	(calc)		
0	—	100	1	108,9		70,8		
1	—	—	1	73,9	—	29,4	0,0	—
7	1,5	5	1	79,3	—	28,6	27,5	—
11a	2,5	5	1	82,7		28,4	27,2	—
17	4	—	1	76,9	118,4	23,7	28,2	4,2
14a	4	2,5	1	73,0	—	28,7	27,5	—
15a	4	5	1	74,5	—	26,5	26,8	—
16	4	7,5	1	80,7	—	27,9	26,0	—
22a	4	5	1	79,0	—	26,9	26,8	—
11b	2,5	5	3	83,2	—	27,6	27,2	—
14b	4	2,5	3	72,2	—	26,3	27,5	—
15b	4	5	3	74,9	—	27,5	26,8	—
22b	4	5	3	80,1		28,0	26,8	—

Sample: 0 is compatibilizer alone. 1 is a near sPP. Nanocomposites marked with *contain compatibilizer iPP-g-MA having higher molecular weight (HC5).

All other samples in Table 1 contain compatibilizer iPP-g-MA with lower molecular weight (AR504).

better dispersion was achieved and experimental ΔH_c values were closer to the calculated ones (Table 3).

The thermograms in Figure 3 show the second annealing of sPP nanocomposites with the same content of filler M-ODA, and with different content of the compatibilizer. The differences between the values of $\Delta H_{c \text{ exp}}$ of samples originated from fibers prepared at $\lambda = 1$ and $\lambda = 3$ indicates that some structural features of the original system remain preserved after melting in DSC pan.

The double peak of the second annealing in the temperature region $T_{m2} = 114\text{--}128^\circ\text{C}$, evidenced polymorphism in sPP [14]. The appearance of these peaks in Figure 4 can be interpreted in two ways. The first one assumes a formation of two different crystalline modifications, the second one assumes an appearance of crystalline modification I, possessing crystals of different sizes that melt at two different temperatures [14]. At lower temperatures the primary (smaller) crystals melt and at higher temperature the same crystals re-crystallize during annealing (to form larger crystals). The size and shape of the double peak depends on the crystallization temperature. With an increase of crystallization temperature the decreased size of the peak proves lower melting enthalpy, and on the contrary,

the peak having higher melting temperature is getting smaller (Figure 3) [8].

Experimentally determined temperatures and enthalpies of melting at the first and second annealing of the sPP nanocomposite samples indicated that during spinning the melting temperatures of PP nanocomposites did not shift to higher values (Tables 3 and 4). Also, there were no significant changes of melting enthalpies, as would be expected from this process. The supermolecular structure of nanocomposite sPP

TABLE 4 Melting Temperatures and Enthalpies of the Selected Nanocomposite Fibers at the Second Annealing

Sample No.	M-ODA wt%	iPP-g-MA wt%	Drawing ratio λ	A		B			
				T_{m2} °C		ΔH_{m2} , J.g ⁻¹			
				1(exp)		1(calc)	2(exp)	2(calc)	
0	—	100		143,3 152,6	72,3				
1	—	—	1	114,9 127,8	158,5	28,1	—	0,04	—
7	1,5	5	1	116,4 128,3	149,9	26,1	26,3	0,4	0,037
11a	2,5	5	1	117,5 128,4	152,0	27,0	26,0	1,5	0,037
17	4	—	1	115,5 127,9	160,7	17,7	27,0	5,6	0,038
14a	4	2,5	1	114,1 127,6	159,6	25,7	26,3	0,5	0,037
15a	4	5	1	114,8 127,7	150,9	24,8	25,6	0,5	0,036
16	4	7,5	1	117,4 128,3	153,1	24,8	24,9	0,9	0,035
22a	4	5	1	117,2 129,0	152,1	20,1	25,6	1,0	0,036
11b	2,5	5	3	118,1 128,6	153,1	26,2	—	2,7	—
14b	4	2,5	3	114,7 127,8	153,1	25,7	—	0,6	—
15b	4	5	3	115,2 127,8	150,8	24,5	—	0,6	—
22b	4	5	3	116,7 128,4	150,8	24,5	—	1,0	—

Sample: 0 is compatibilizer alone. 1 is a near sPP. Nanocomposites marked with *contain compatibilizer iPP-g-MA having higher molecular weight (HC5).

All other samples in Table 1 contain compatibilizer iPP-g-MA with lower molecular weight (AR504).

fibers, which arose during the technological fiber-forming process, was a product of one-directional deformation-elongation.

Sample 22a containing HC5, the compatibilizer with a higher molar mass, crystallized at higher temperature than sample 15 containing a compatibilizer AR504 with lower molar mass (Table 3). The higher crystallization temperature of the HC5 influenced the melting temperature T_{m2} of the second annealing of sample 22a, which slightly increased in comparison with sample 15 containing compatibilizer AR504 (Table 4).

The processes of repeated melting and crystallization of sPP nanocomposites of constant content of compatibilizer AR504 (5 wt%) and different content of the filler M-ODA (1.5; 2.5 and 4 wt%) are illustrated in Figures 1 and 3. The shapes of the thermograms for sPP nanocomposite fibers corresponded to the thermal behavior of neat sPP. Changing amount of M-ODA while maintaining constant amount

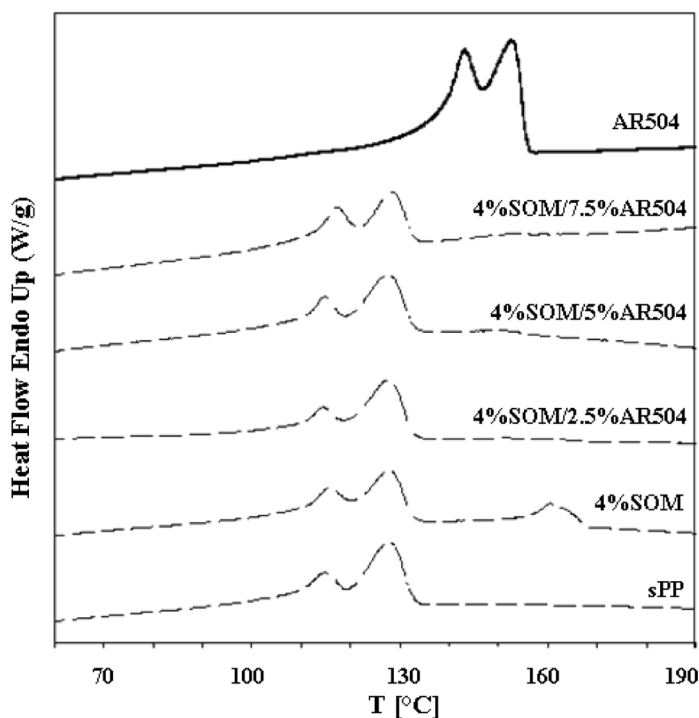


FIGURE 4 DSC Melting Thermograms of: sPP without Additives; Compatibilizer AR504 and sPP Nanocomposites with constant content of the filler M-ODA = 4wt% and with various content of the compatibilizer AR504 (2.5; 5 and 7.5 wt%) at the second annealing.

of compatibilizer brought about only slight variation of temperature and enthalpy of melting.

Increased content of M-ODA caused slight increase in both melting and crystallization temperatures (Figures 5, and 6). But the peaks characterizing the sPP crystallization in the corresponding nanocomposites sPP systems were higher and narrower than peaks obtained for the neat sPP. This indicated the formation of a more uniform size of sPP crystals (Figure 3).

The thermograms of the second annealing of sPP nanocomposite samples with increasing content of the filler and constant content of compatibilizer (Figure 6) do not differ from the thermograms of the first annealing of sPP nanocomposites, compare Figure 4. Transition of the simple major sPP peak of the first annealed thermogram in the melting temperature region, 125–127°C, into the double peak in the same melting temperature region is caused by the different

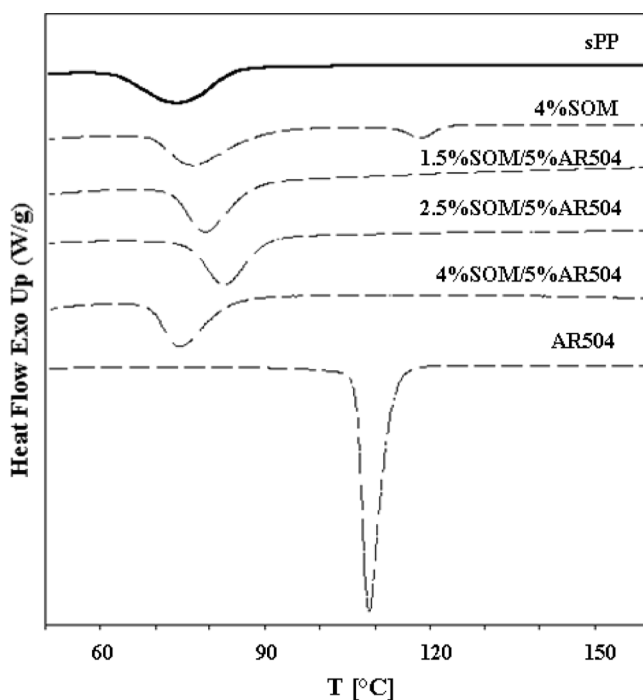


FIGURE 5 DSC thermograms of sPP nanocomposite samples containing various amount of filler M-ODA (1.5; 2.5; and 4 wt%) and constant content of compatibilizer AR504 = 5 wt% at cooling (crystallization) and thermograms of unfilled sPP and compatibilizer AR504 alone.

formation of the super-molecular structure of the fibers and non-oriented sPP nanocomposite system.

The addition of 4 wt% of the filler did not increase the melting temperature of the sPP and its crystalline content. The crystalline content in the nanocomposite without compatibilizer was lower than the calculated one (Table 5), which corresponds to the content of neat sPP in the sPP nanocomposite. The same tendency was observed for sPP nanocomposites prepared in presence of the compatibilizer (Table 5).

The presence of compatibilizer HC5, with the higher molar mass, gave a lower crystalline peak in sPP nanocomposite fibers than the presence of compatibilizer AR504, with lower molar mass.

A comparison of the sPP nanocomposite fibers prepared at $\lambda = 1$ drawing ratio with non-spun sPP nanocomposite showed that the

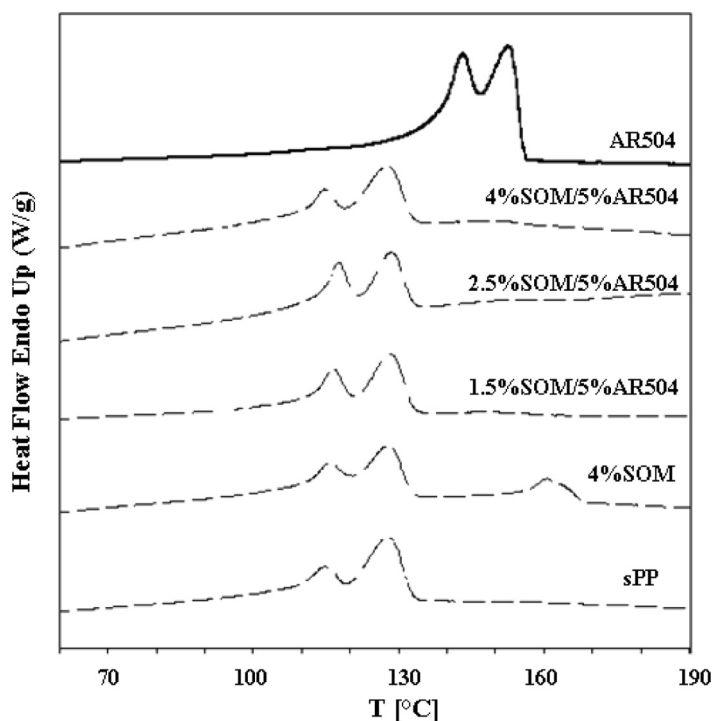


FIGURE 6 DSC thermograms of the second annealing of the sPP nanocomposite samples with various content of filler (1.5; 2.5 and 4 wt%) and constant content of compatibilizer AR 504 = 5 wt%, thermograms of unfilled sPP and compatibilizer AR 504.

TABLE 5 Crystallinity (Cryst.) of the Selected Nanocomposite Fibers at the First and Second Annealing

Sample no.	M-ODA wt%	iPP-g-MA wt%	Drawing ratio λ	Cryst. %			
				exp	calc	exp	calc
0	—	100	1	39,7	—	39,5	—
1	—	—	1	15,4	—	15,4	—
7	1,5	5	1	13,6	14,6	14,5	15,5
11a	2,5	5	1	13,6	14,7	15,6	16,8
17	4	—	1	11,6	12,1	12,7	13,3
14a	4	2,5	1	14,9	15,9	14,3	15,3
15a	4	5	1	10,4	11,4	13,8	15,2
16	4	7,5	1	13,2	14,9	14,0	15,9
22a	4	5	1	9,8	10,8	11,5	12,7
11b	2,5	5	3	16,5	17,8	15,8	17,1
14b	4	2,5	3	14,4	15,4	14,4	15,4
15b	4	5	3	13,9	15,3	13,7	15,1
22b	4	5	3	13,1	14,4	13,9	15,3

Sample: 0 is compatibilizer alone. 1 is a near sPP. Nanocomposites marked with * contain compatibilizer iPP-g-MA having higher molecular weight (HC5).

All other samples in Table 1 contain compatibilizer iPP-g-MA with lower molecular weight (AR504).

crystallinity in practically all samples (except for sample 14, Table 5) was lower in spun sPP nanocomposite than in the non-spun samples.

CONCLUSIONS

From this study the following conclusions can be drawn:

- sPP/SOMASIF nanocomposites crystallized mostly in the structural modification II and less frequently in modification III. Formation of the modification III is helped by the facilitated nanofiller M-ODA.
- Melting temperatures of all spun sPP/M-ODA nanocomposite fibers showed higher melting temperatures than the neat sPP fibers. The higher and narrower shape of the sPP peak in the nanocomposite system indicated formation of sPP crystals with narrower size distribution. That was most probably the reason for the melting temperature increase of the sPP/M-ODA nanocomposite fibers.
- The crystalline fraction of sPP matrix of all investigated sPP/M-ODA nanocomposite fibers was lower than in the neat sPP fibers. This holds for the crystalline part, which was obtained after second annealing of nanocomposite fibers. This observation could

be explained as a result of competition between formation of physical network in amorphous part of the sPP matrix, caused by filler, and crystallization of sPP chains in the crystalline part.

- The increase of drawing ratio of sPP/M-ODA nanocomposite fibers allowed attainment of a slightly higher amount of sPP crystalline part in the sPP matrix.

REFERENCES

- [1] Kaempfer, D., Thomann, R., and Mülhaupt, R., *Polymer* **43**, 2909 (2002).
- [2] Mlynarcikova, Z., Kaempfer, D., Thomann, R., Mülhaupt, R., Borsig, E., and Marcincin, A., *Polym. Adv. Technol.* **16**, 362 (2005).
- [3] Natta, G., Pasquon, J., Corradini, P., Peraldo, M., Pegararo, M., and Zambelli, A., *Accad. Nar. Lincei Rend Classe Sci Fis. Mat. Nat.* **28**, 539 (1960).
- [4] Loos, J., Buhk, M., Petermann, J., Zoumis, K., and Kaminsky, W., *Polymer* **37** (3), 387 (1996).
- [5] Uehara, H., Yamazaki, Y., and Kanamoto, T., *Polymer* **37** (1), 57 (1996).
- [6] Heck, B., Hugel, T., Iijima, M., and Strobl, G., *Polymer* **41**, 8839 (2000).
- [7] Supaphol, P., and Spruiell, J. E., *Polymer* **41**, 1205 (2000).
- [8] Supaphol, P., and Spruiell, J. E., *Polymer* **42** (2), 699 (2001).
- [9] Supaphol, P., and Lin, J. -S., *Polymer* **42**, 9617 (2001).
- [10] De Rosa, C., and Auriemma, F., de Ballesteros, O. R., *Polymer* **42**, 9729 (2001).
- [11] Hahn, T., Suen, W., Kang, S., Hsu, S. L., Stidham, H. D., and Siedle, A. R., *Polymer* **42**, 5813 (2001).
- [12] Thomann, R., Wang, C., Kressler, J., Juengling, S., and Mülhaupt, R., *Polymer* **36**, 3795 (1995).
- [13] Sevegney, M. S., Parthasarthy, G., Kannan, R. M., Thurmman, W. D., and Fernandez-Ballester, L., *Macromolecules* **36**, 6472 (2003).
- [14] Lotz, B., Mathieu, C., Thierry, A., Lovinger, A. J., De Rosa, C., de Ballesteros, O. R., and Auriemma, F., *Macromolecules* **31** (26), 9253 (1998).
- [15] Men, Y., and Strobl, G., *J. of Macromol. Sci.—Physics* **B40** (5), 775 (2001).
- [16] Mouzakis, D. E., Kandilioti, G., Elenis, A., Gregoriou, V. G., *J. Macromol. Sci., Part A*, **43**, 259 (2006).
- [17] Saujanya, C., and Radhakrishnan, S. *Polymer* **42**, 6723 (2001).
- [18] Sozzani, P., Simonutti, R., and Galimberti, M., *Macromolecules* **26**, 5782 (1993).
- [19] Charitani, Y., Maruyama, H., and Nogochi, K., *J. Polymer Sci, C* **28**, 393 (1990).